

# Modeling Helicopter Rotor Blade Flapping Motion Considering Nonlinear Aerodynamics

Jyoti Ranjan Majhi, Ranjan Ganguli<sup>1</sup>

**Abstract:** The flapping equation for a rotating rigid helicopter blade is typically derived by considering 1) small flap angle, 2) small induced angle of attack and 3) linear aerodynamics. However, the use of nonlinear aerodynamics can make the assumptions of small angles suspect. A general equation describing helicopter blade flap dynamics for large flap angle and large induced inflow angle of attack is derived in this paper with nonlinear aerodynamics. Numerical simulations are performed by solving the nonlinear flapping ordinary differential equation for steady state conditions and the validity of the small angle approximations are examined. It is shown that the small flapping assumption, and to a lesser extent, the small induced angle of attack assumption can lead to inaccurate predictions of the blade flap response in certain flight conditions for some rotors when nonlinear aerodynamics is considered.

**Keyword:** Helicopter, Flapping, Aerodynamics, Aeroelasticity, Nonlinear System, Fluid-Structure Interaction

## 1 Introduction

Helicopter blades undergo flap, lag and twist motions. The out-of-plane motion of the blade is called flap and the in-plane motion is called lag. The simplest model of a rotating blade involves a rigid blade hinged at the root and undergoing flapping motion due to the effect of centrifugal, inertia and aerodynamic forces, as shown in Fig.1. Accurate solution of the flapping equation provides basic insights into helicopter rotor dynamics.

The flapping equation is derived in terms of co-

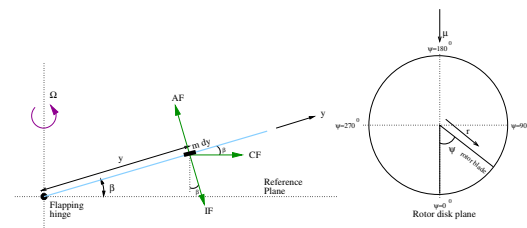


Figure 1: Forces acting on an element of a flapping blade

ordinates  $r$  (radial distance from the root) and  $\psi$  (azimuth angle) shown in Fig.1. In hover, the flap angle is constant throughout the azimuth because of axisymmetric aerodynamic loading. But, in forward flight this axisymmetry is lost and the aerodynamic load is a function of azimuth and radial distance from the root and the flap angle essentially varies with the azimuth in a periodic manner. The aerodynamic loading depends upon the pitching angle of the blade as well as the inflow through the rotor disk and so does the flap angle. The pitch angle,  $\theta(\psi)$ , shown in Fig.2, is the pilot control input and the inflow,  $\phi$ , is due to the velocity  $U_P$  in the downward direction. The rotor blade section thus experiences an effective angle of attack given by,  $\alpha = \theta - \phi$ .

The flapping equation with small flap angle assumption is derived in Leishman (1992) and Johnson (1975) which need not be applicable in high angle of attack regime because of the nonlinearities involved. In these derivations, the assumption is made that  $\beta$  and  $\phi$  are small angles.

Considerable research over the past two decades has shown that aeroelastic nonlinearities play an important role in fixed-wing (Librescu, Chiochia, and Marzocca (1995); Chandiramani, Plaut, and Librescu (1996); Patil and Hodges

<sup>1</sup> Department of Aerospace Engineering, Indian Institute of Science, Bangalore-560012, India

(2004); Tang and Dowell (2004); Kamakoti, Lian, Regisford, and et al. (2002)) and helicopter rotor aeroelasticity (Tongue and Flowers (1988); Desceliers and Soize (1999); Cesnik, Opoku, Nitzsche, and Cheng (2004); Simonetti and Marretta (2000)). These nonlinearities can be broadly classified into structural and aerodynamic categories. Tang and Dowell (1993), Dowell (1990), and Dowell and Ilgamov (1988) have given detailed accounts on the aeroelastic nonlinearities. In general, nonlinearities can significantly affect the behavior of a dynamical system (Christov, Christov, and Jordan (2007); Liu (2006); Wachter and Givoli (2006); Leu and Chen (2006); Han, Rajendran, and Atluri (2005)). However, in helicopter dynamics, an elastic blade model is often used resulting in a proliferation of moderate and large deflection geometric nonlinearity terms in addition to coriolis terms due to flap-lag coupling.

In the present work, a general flapping equation is derived without any linearization of the aeroelastic nonlinearities and it is shown that the corresponding equation for small flap angles given in text books can be obtained as a special case of this equation. Then the validity of the small flap angle and inflow angle approximation is investigated assuming nonlinear aerodynamics. Interestingly, some of these small angle assumptions are shown to be inappropriate at certain flight conditions but are often made in aeroelastic codes.

## 2 Blade Element Analysis

The blade element theory is used to obtain the loads acting on a blade section. At any element at a radial station  $r$  and azimuth angle  $\psi$ , the blade cross-section consists of an airfoil section as shown in Fig.2. The assumptions of small  $\beta$  and  $\phi$  are not made in the derivations shown below.

### 2.1 Blade Element Velocity Components

There are three components of velocity, an in-plane component of velocity,  $U_T$ , an out-of-plane component,  $U_P$  and a radial component,  $U_R$  given

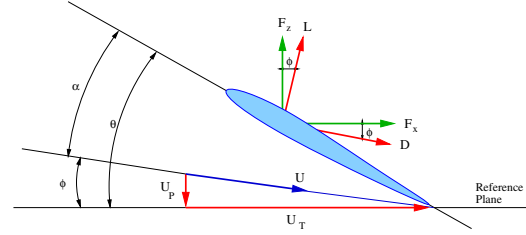


Figure 2: Blade element velocities and forces

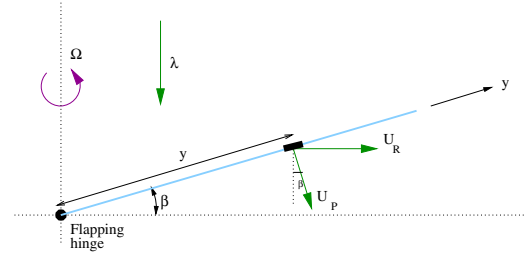


Figure 3: Blade element velocities resulting from flapping

by(see Fig.2 and Fig.3),

$$U_R = (\Omega R)\mu \cos \psi \quad (1)$$

$$U_T = (\Omega R)(r \underline{\cos \beta} + \mu \sin \psi) \quad (2)$$

$$U_P = (\Omega R)(\lambda \underline{\cos \beta} + r \beta^* + \mu \underline{\sin \beta} \cos \psi) \quad (3)$$

where  $\mu = \frac{V_\infty \cos \alpha_s}{\Omega R}$  is the advance ratio, where  $\alpha_s$  is the rotor disk angle of attack and  $\lambda$  is the rotor disk induced inflow ratio. The underlined  $\cos \beta$  and  $\sin \beta$  terms occur because we have not assumed that  $\beta$  is small.

### 2.2 Blade Element Forces

Lift and drag forces per unit blade span are given by,

$$L = \frac{1}{2} \rho U^2 c C_L \quad (4)$$

$$D = \frac{1}{2} \rho U^2 c C_D \quad (5)$$

where,

$$U = \text{resultant velocity} = \sqrt{U_T^2 + U_P^2}$$

$$C_L = C_L(\alpha)$$

$$C_D = C_D(\alpha)$$

and

$$\begin{aligned} \alpha &= \theta - \phi = \theta - \arctan \frac{U_P}{U_T} \\ &= \theta_0 + \theta_{1c} \cos \psi + \theta_{1s} \sin \psi \\ &\quad - \arctan \frac{\lambda \cos \beta + r\beta + \mu \sin \beta \cos \psi}{r \cos \beta + \mu \sin \psi} \end{aligned} \quad (6)$$

where the expressions for  $U_T$  and  $U_P$  in Eq.2 and 3 have been used. The lift and drag forces act perpendicular and parallel respectively to the direction of the resultant flow velocity,  $U$ . The normal force acting on the rotor disk is then given by,

$$F_z = \underline{L} \cos \phi - \underline{D} \sin \phi \quad (7)$$

where again the small  $\phi$  assumption is not used as indicated by the underlined terms.

### 3 Flapping Equation

Considering a rigid articulated rotor blade with no flap hinge offset, the forces acting on an element of mass  $mdy$  are (see Fig.1),

1. Inertia force (IF) =  $(mdy)\ddot{\beta}y$ , opposing the flapping motion;
2. Centrifugal force (CF) =  $(mdy)\Omega^2(y \cos \beta)$ , acting radially outwards; and
3. Aerodynamic force (AF) =  $F_z dy$ , normal to the blade.

The moment equilibrium of the above forces gives,

$$\begin{aligned} &\int_0^R [(mdy)\ddot{\beta}y]y + \int_0^R [(mdy)\Omega^2(y \cos \beta)](y \sin \beta) \\ &= \int_0^R [F_z dy]y \end{aligned} \quad (8)$$

$$\text{i.e. } I_b(\ddot{\beta} + \Omega^2 \cos \beta \sin \beta) = \int_0^R F_z y dy \quad (9)$$

$$\text{i.e. } \beta + \underline{\cos \beta \sin \beta} = \frac{R}{\Omega^2 I_b} \int_0^1 F_z r dr \quad (10)$$

The above equation is the general flapping equation for a simple articulated rotor blade with no flap hinge offset and with no spring restraint where  $F_z$  is defined in Eq.7. We note that at

this point we have not made any assumption regarding aerodynamic nonlinearity in terms of  $C_L$  and  $C_D$ . However, Eq.10 is nonlinear in  $\beta$  and  $\psi$ .

The flapping equation for small flap angles [Appendix] can be easily deduced from this equation by substituting,  $\cos \beta = 1$ ,  $\sin \beta = \beta$  and  $F_z = L \cos \phi - D \sin \phi \approx L$ .

### 4 Aerodynamics model

To model the aerodynamic behavior of the rotor system in all flight regimes accurately is a difficult task because of the highly complicated nature of the unsteady aerodynamic effects. At low angles of attack with fully attached flow, the unsteadiness is moderate and can be modeled with quasi-steady approximations without much difficulty. For linear aerodynamics, the aerodynamic loads on an airfoil at low angles of attack can be modeled as polynomial functions of the angle of attack by curve fitting the airfoil test data. Airfoil test data for commonly used airfoils are available in Abbott and Doenhoff Abbott and von Doenhoff (1949) and airfoil data for any other specific airfoil can be obtained by CFD simulation or wind tunnel tests. The typical linear aerodynamic model used in deriving the flap equation is

$$C_L(\alpha) = a_0 + a_1 \alpha \quad (11)$$

$$C_D(\alpha) = d_0 + d_1 \alpha + d_2 \alpha^2 \quad (12)$$

where  $a_0$ ,  $a_1$ ,  $d_0$ ,  $d_1$  and  $d_2$  are constants. These models are valid until static stall is reached.

But in high angle of attack regimes, the lift and drag become highly nonlinear functions of the angle of attack, due to separation and stall. The purpose of this study is to investigate the validity of the small  $\beta$  and small  $\phi$  assumptions in the flapping equation. For this purpose, a linear aerodynamics model shown in Eq.11 and 12 is inappropriate as it is valid only for low  $\alpha$  which may not result in all flight conditions of the helicopter. There are two simple methods to account for high angle of attack aerodynamics. The first method used for rotor analyses is the table look-up method in which the section airloads

at different values of angle of attack are tabulated against the corresponding angle of attacks from airfoil test data and an interpolating technique is used for intermediate values. The second method is based on curve fits using data which is valid between angles of attack of  $-180^0$  and  $180^0$ . In the high angle of attack range, airloads can be modeled as smooth curves by the quasi-steady approximation Leishman (1992) as,

$$C_L(\alpha) = A \sin 2(\alpha - \alpha_0) \quad (13)$$

$$C_D(\alpha) = D + E \cos 2(\alpha - \alpha_0) \quad (14)$$

where  $A = 1.1$  for NACA 0012 airfoil and  $A = 1.25$  for the SC 1095 airfoil, for any arbitrary airfoil the average value of both the airfoils works reasonably and  $D = 1.135$  and  $E = -1.05$  work well for any arbitrary airfoil. In this paper, we consider a NACA 0012 airfoil.

### 5 Results and Discussion

The blade can be visualized as a composite of a number of aerodynamic sections situated at different radial distances from the flap hinge. Considering a blade element of sufficiently small span  $\Delta r$  situated at  $r_0$  nondimensional distance from the flap hinge as shown in Fig.4, the airloads can be assumed to be independent of  $r$  over this span, i.e.  $F_z = F_z(\psi)$ . The flapping equation for this el-

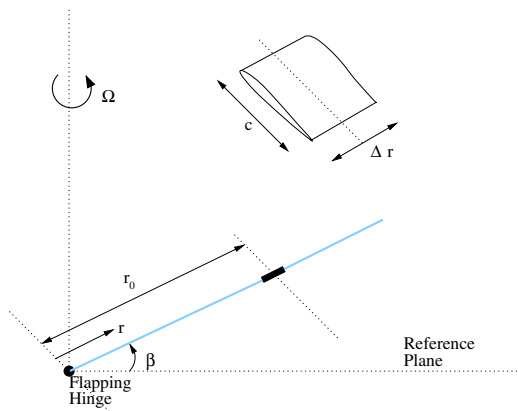


Figure 4: Forces acting on an element of a flapping blade

ement can then be derived in the way it is carried

out in Sec.4 (Eq.8-10) as  
Large  $\beta$  formulation :

$$\beta + \cos \beta \sin \beta = \frac{R}{\Omega^2 I_{\Delta r}} F_z(\psi) r_0 \Delta r \quad (15)$$

Small  $\beta$  formulation :

$$\beta + \beta = \frac{R}{\Omega^2 I_{\Delta r}} F_z(\psi) r_0 \Delta r \quad (16)$$

where  $I_{\Delta r}$  is the moment of inertia of the blade element about the flap hinge.

#### 5.1 Solution Procedure

The above flapping equation for the blade element is a second order ordinary differential equation in  $\beta$ . This is solved using a Runge-Kutta technique with zero initial conditions. Transients are allowed to decay and the final blade steady response  $\beta(\psi)$  is considered.

A blade element of span  $\Delta r = 0.02$ , i.e. the blade is divided into fifty blade elements and one among those is chosen, at  $r_0 = 0.75$  and the flapping response, the angles of attack and lift coefficient are found out. Static aerodynamics based on Eq.11-14 is used. The results presented here are carried out with the following data of a four bladed rotor:

Blade Data	
$\mu = 0.3$	
$R = 8.17$ m	
$c = 0.5273$ m	
$m = 13.04651163$ kg/m	
$C_T/\sigma = 0.0726$	
rotor disk angle of attack $\alpha_s = 15^0$	
Airfoil section (NACA 0012) characteristics:	
$C_L = \begin{cases} 6.25\alpha & \text{for }  \alpha  < \alpha_{stall} = 13^0 \\ 1.1 \sin 2(\alpha - \alpha_0) & \text{for }  \alpha  > \alpha_{stall} = 13^0 \end{cases}$	
$C_D = \begin{cases} 0.006 + 0.005 C_L^2 & \text{for }  \alpha  < \alpha_{stall} = 13^0 \\ 1.135 - 1.05 \cos 2(\alpha - \alpha_0) & \text{for }  \alpha  > \alpha_{stall} = 13^0 \end{cases}$	
$\alpha_0 = 0^0$	

In Fig.5-8 a typical set of results with the large  $\beta$  and large  $\phi$  formulation with a uniform inflow

model for only a collective pitch input of  $\theta_0 = 13^\circ$  is presented.

The main objective of this paper is to address two issues, 1) the validity of the small  $\beta$  assumption, and 2) the validity of the small  $\phi$  assumption. These assumptions are investigated in the foregoing subsections.

### 5.2 Flapping Response

The flapping responses with the proposed formulation (large  $\beta$  and large  $\phi$ ) are presented here along with those derived from the small angle approximation formulation (small  $\beta$  and large  $\phi$ ), see Fig.9-16.

In both of the cases a uniform inflow model is used. We see that as  $\theta_0$  increases from  $1^\circ$  to  $20^\circ$  in Fig.9 through Fig.16, the small  $\beta$  assumption becomes incorrect. For low  $\theta_0$  the effect is primarily on the magnitude of the flap response but at higher  $\theta_0$ , it affects both magnitude and phasing.

### 5.3 Induced Inflow Angle

As shown above, the small flap angle approximation formulation is not always valid. In general, for high angle of attack aerodynamics problems, the model proposed in this paper can be used. Note that in Fig.9 through Fig.16,  $\phi$  is assumed to be large. It is important to investigate the nature of the induced inflow angle, that is, whether it is really large or a small angle approximation can be made which might lessen the mathematical complication of the model. As can be seen from Eq.6 and 7, the assumption of large  $\phi$  results in a complicated formulation. To verify this, the variation of the induced inflow angle is calculated here from the proposed model with the usual induced inflow angle,  $\phi = \arctan \frac{U_p}{U_T}$  as well as that with small angle approximation, i.e.,  $\phi = \frac{U_p}{U_T}$  in different flight regimes as follows.

#### 5.3.1 Induced inflow angle for uniform inflow model

The results presented here are calculated using a uniform inflow model.

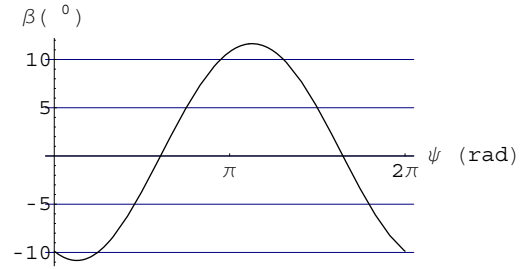


Figure 5: Flapping response

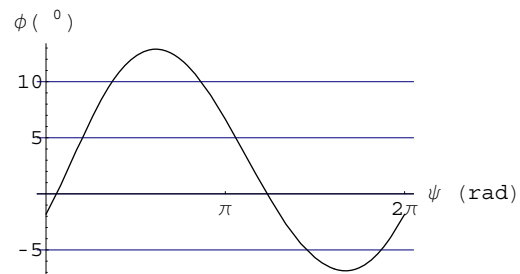


Figure 6: Induced inflow angle of attack

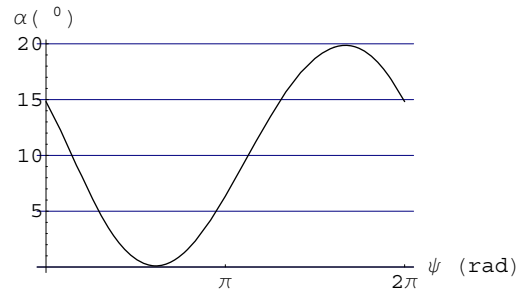


Figure 7: Total effective angle of attack

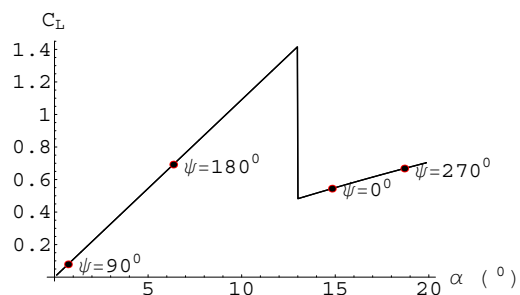


Figure 8: Lift coefficient

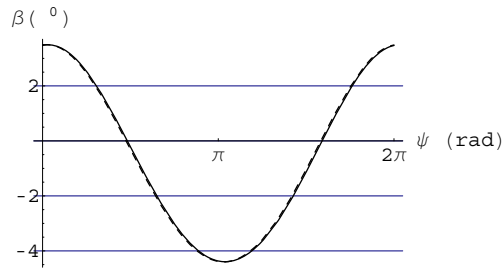


Figure 9:  $\theta_0 = 1^\circ$

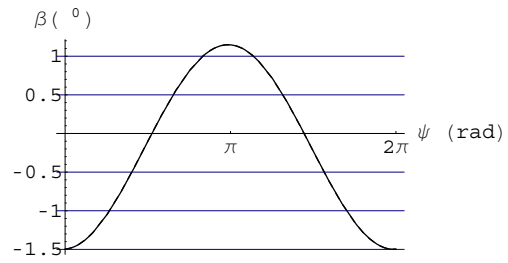


Figure 10:  $\theta_0 = 5^\circ$

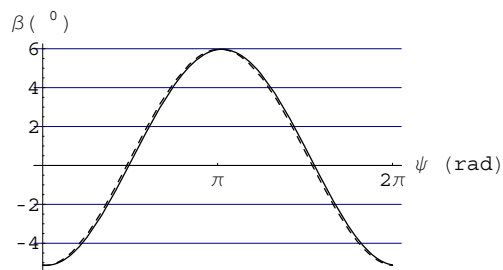


Figure 11:  $\theta_0 = 10^\circ$

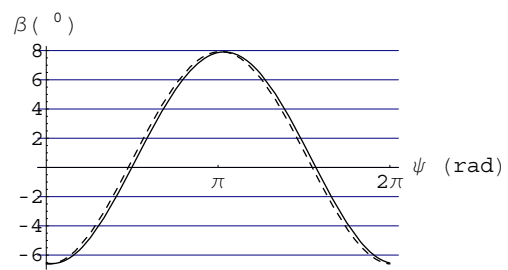


Figure 12:  $\theta_0 = 12^\circ$

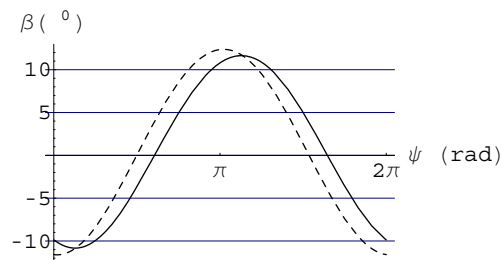


Figure 13:  $\theta_0 = 13^\circ$

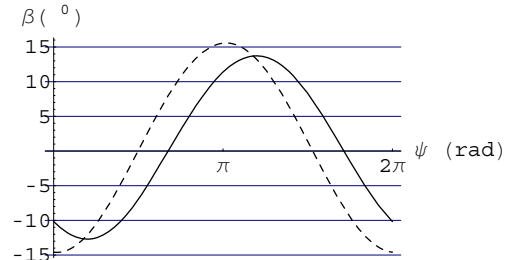


Figure 14:  $\theta_0 = 15^\circ$

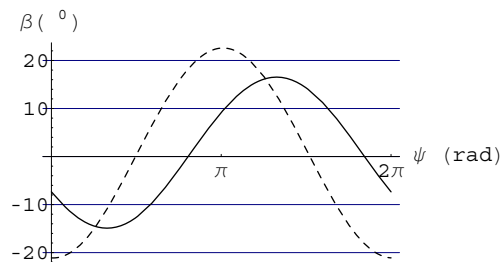


Figure 15:  $\theta_0 = 17^\circ$

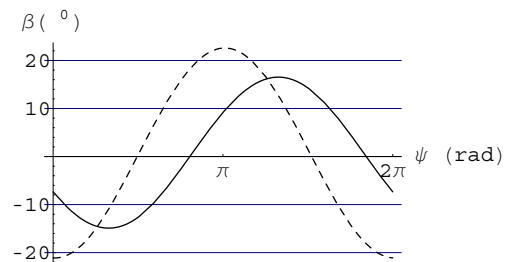


Figure 16:  $\theta_0 = 20^\circ$

Fig.9-16. Variation of  $\beta$  with Azimuth. \_\_\_\_\_ large  $\beta$  large  $\phi$ ; - - - - - small  $\beta$  large  $\phi$ .

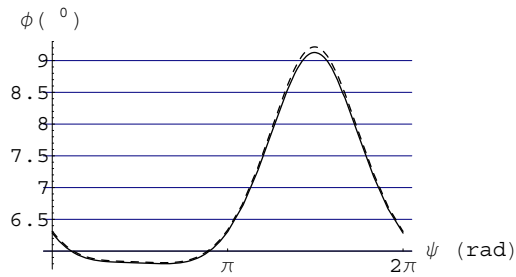


Figure 17:  $\theta_0 = 5^0$

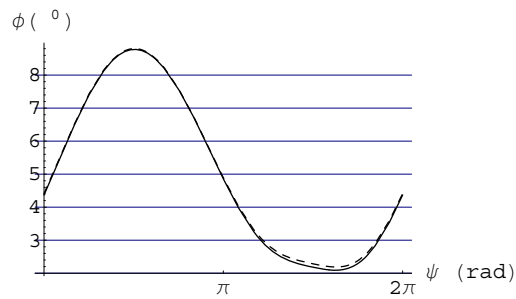


Figure 18:  $\theta_0 = 10^0$

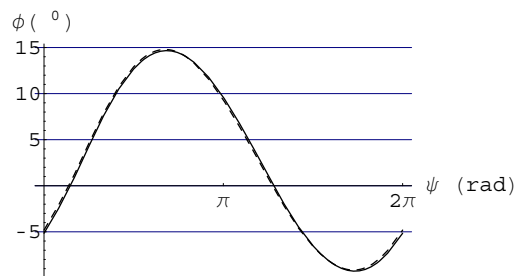


Figure 19:  $\theta_0 = 15^0$

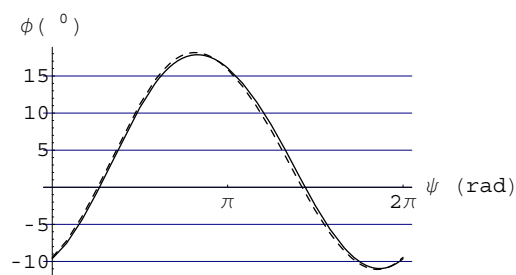


Figure 20:  $\theta_0 = 20^0$

Fig.17-20. Variation of  $\phi$  with Azimuth. \_\_\_\_\_ large  $\beta$  large  $\phi$ ; - - - - large  $\beta$  small  $\phi$ .

We can conclude (from Fig.17-20) that for a uniform inflow model and collective pitch  $\theta_0$  input the small  $\phi$  approximation holds good.

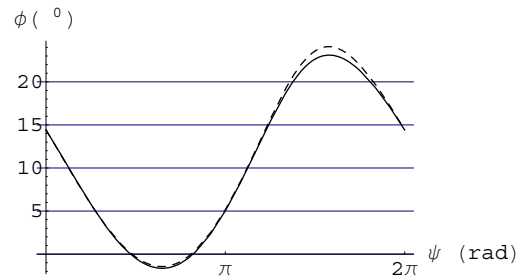


Figure 21:  $\theta_0 = 8^0, \theta_0 = 4^0, \theta_0 = -10^0$

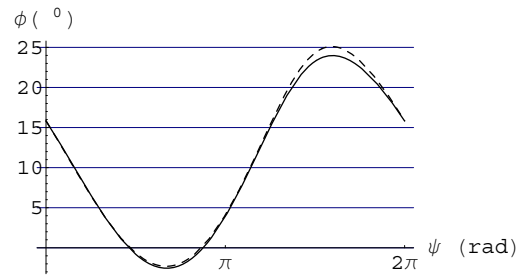


Figure 22:  $\theta_0 = 10^0, \theta_0 = 5^0, \theta_0 = -12^0$

Fig.21-22. Variation of  $\phi$  with Azimuth. \_\_\_\_\_ large  $\beta$  large  $\phi$ ; - - - - large  $\beta$  small  $\phi$ .

Also this assumption is investigated for typical cases of cyclic pitch inputs (Fig.21-22) and it is observed that the angle is altered by about  $1 - 2^0$  near  $\psi = 3\pi/2$ , which is significant.

### 5.3.2 Induced inflow angle for uniform inflow model with large disk loading

Next, let us see whether this assumption can be made for a large disk loading. For this a  $\frac{C_T}{\sigma}$  as high as 0.15 is chosen and the induced inflow angle is simulated for  $\mu = 0.3$  as well as for  $\mu = 0.4$ . The results are presented in Fig.23 through Fig.28.

We see that the small induced inflow angle of attack assumption can be made even for extreme

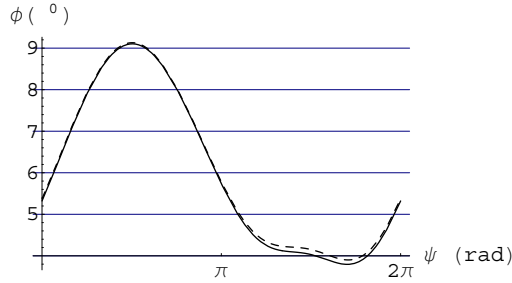


Figure 23:  $\theta_0 = 10^0, \mu = 0.3$

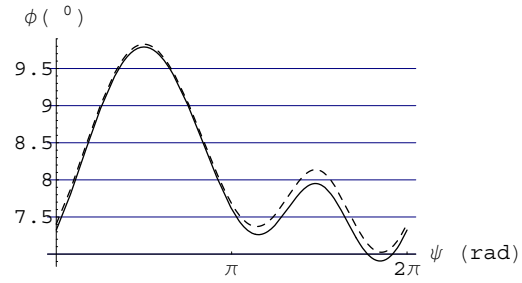


Figure 25:  $\theta_0 = 10^0, \mu = 0.4$

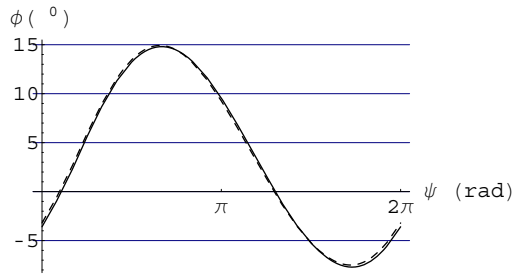


Figure 24:  $\theta_0 = 15^0, \mu = 0.3$

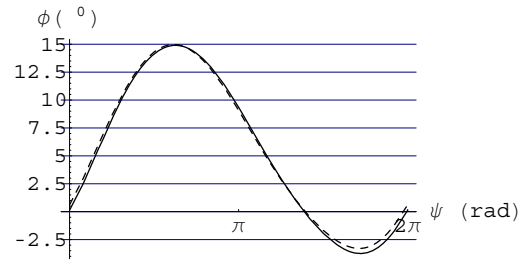


Figure 26:  $\theta_0 = 15^0, \mu = 0.4$

Fig.23-24. Variation of  $\phi$  with Azimuth for  $\frac{C_T}{\sigma} = 0.15$ . \_\_\_\_\_ large  $\beta$  large  $\phi$ ; - - - - large  $\beta$  small  $\phi$ .

Fig.25-26. Variation of  $\phi$  with Azimuth for  $\frac{C_T}{\sigma} = 0.15$ . \_\_\_\_\_ large  $\beta$  large  $\phi$ ; - - - - large  $\beta$  small  $\phi$ .

disk loading in cases where only collective pitch is applied. But when cyclic pitch is also applied this assumption does not hold true as it is seen from Fig.27-28.

$$U_P = (\Omega R)(\lambda \cos \beta + r\beta^* + \mu \sin \beta \cos \psi) + V_c \tag{19}$$

$$\phi = \arctan \frac{(\Omega R)(\lambda \cos \beta + r\beta^* + \mu \sin \beta \cos \psi) + V_c}{(\Omega R)(r \cos \beta + \mu \sin \psi)} \tag{20}$$

### 5.3.3 Induced inflow angle for linear inflow model in climbing forward flight with varying cyclic pitch and rotation speed

The above results were restricted in terms of flight conditions and wake models. Looking at the expression of the induced inflow angle (Eq.6) it can be suspected that it could be high at certain azimuth locations in the case of a linear inflow model. In addition, a climb speed,  $V_c$  is considered. Here, we have,

$$\lambda = \lambda_0(1 + k_r r \cos \psi) \tag{17}$$

$$U_T = (\Omega R)(r \cos \beta + \mu \sin \psi) \tag{18}$$

To simulate this a  $k_r$  of 1.2 and a climb speed of 15 m/sec is chosen and  $\phi$  is calculated from the proposed model with and without considering the small  $\phi$  assumption. There could be many combinations of the collective, lateral cyclic and longitudinal cyclic pitches which would give rise to a large induced inflow angle; also a small rotational speed could lead to a large induced inflow angle. Results for several combinations are presented in Fig.29 through Fig.32. From Fig.29-30, it is observed that even when only collective pitch is applied the small  $\phi$  assumption is not appropriate to an appreciable extent.



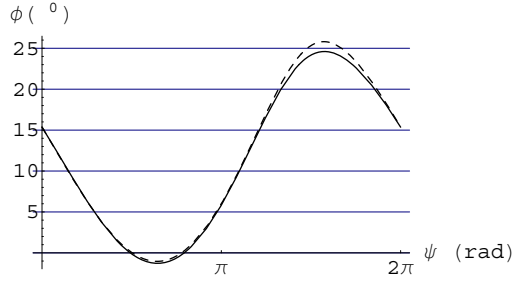


Figure 27:  $\mu = 0.3$

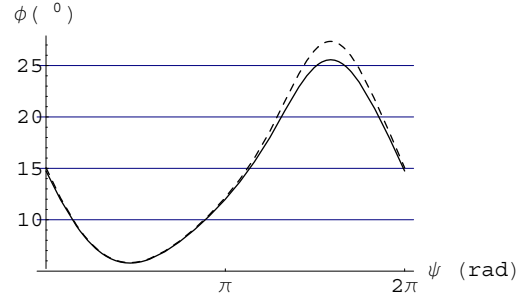


Figure 29:  $\theta_0 = 5^0$

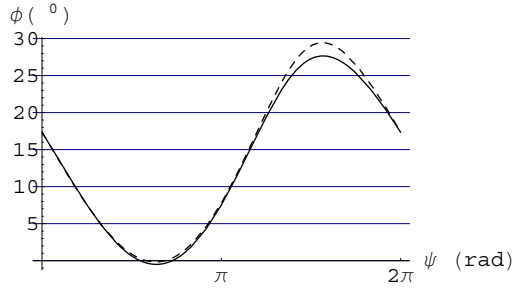


Figure 28:  $\mu = 0.4$

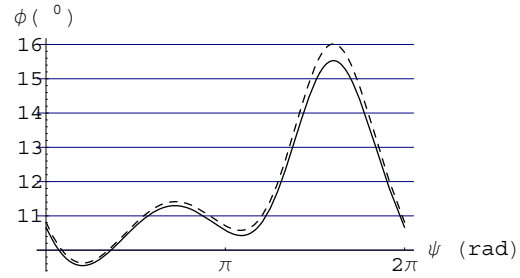


Figure 30:  $\theta_0 = 10^0$

Fig.27-28. Variation of  $\phi$  with Azimuth for  $\frac{C_T}{\sigma} = 0.15$ ,  $\theta_0 = 8^0$ ,  $\theta_{1c} = 4^0$ ,  $\theta_{1s} = -10^0$ . \_\_\_\_\_ large  $\beta$  large  $\phi$ ; - - - - large  $\beta$  small  $\phi$ .

Fig.29-30. Variation of  $\phi$  with Azimuth for linear inflow in climbing forward flight. \_\_\_\_\_ large  $\beta$  large  $\phi$ ; - - - - large  $\beta$  small  $\phi$ .

And when cyclic pitch inputs are also applied the assumption certainly breaks down as seen from Fig.31-32.

In these cases, small changes in the values of  $\phi$  lead to changes in the blade response. Both magnitude and phasing of the response are affected.

Note that  $\beta^*$  and  $\beta^{**}$  representing damping and inertia forces are important terms in helicopter dynamics and any inaccuracies in the prediction of  $\beta$  also affects these terms to an even greater extent. Therefore, the assumption of small  $\beta$  and small  $\phi$  often made in helicopter flap dynamics may not be appropriate.

## 6 Conclusion

In this article, a general flapping equation is formulated without making small angle assumptions.

A nonlinear aerodynamics model is used. There onwards it is shown that the small flap angle formulation can lead to inaccurate predictions in the flap response. Then the validity of the small induced inflow angle of attack assumption is investigated in various flight regimes and it is seen that in many normal modes of helicopter flight the assumption can be made but in certain high performance operations it is not accurate. Therefore, it is better to assume that the flap angle  $\beta$  and inflow angle  $\phi$  are large angles in helicopter dynamics. The final model of the flapping equation can be summarized as,

$$\beta^{**} + \cos \beta \sin \beta = \frac{R}{\Omega^2 I_b} \int_0^1 F_z r dr \quad (21)$$

$$U_T = (\Omega R)(r \cos \beta + \mu \sin \psi) \quad (22)$$

$$U_P = (\Omega R)(\lambda \cos \beta + r \beta^* + \mu \sin \beta \cos \psi) \quad (23)$$

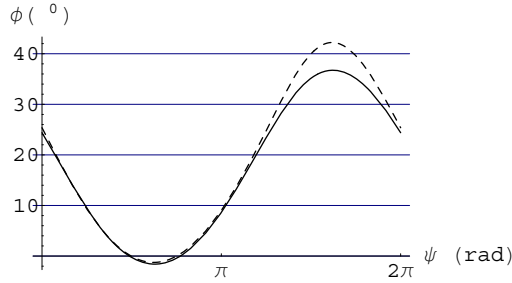
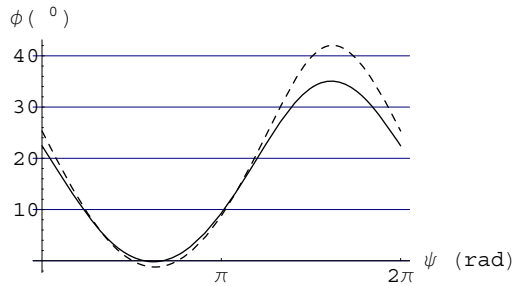
Figure 31:  $\theta_0 = 8^\circ$ ,  $\theta_{1c} = 4^\circ$ ,  $\theta_{1s} = -10^\circ$ Figure 32:  $\theta_0 = 10^\circ$ ,  $\theta_{1c} = 5^\circ$ ,  $\theta_{1s} = -12^\circ$ 

Fig.31-32. Variation of  $\phi$  with Azimuth for linear inflow in climbing forward flight with varying cyclic pitch. ——— large  $\beta$  large  $\phi$ ; - - - - large  $\beta$  small  $\phi$ .

$$\phi = \arctan \frac{U_P}{U_T}; \alpha = \theta - \phi \quad (24)$$

$$F_z = L \cos \phi - D \sin \phi \quad (25)$$

$$L = \frac{1}{2} \rho U^2 c C_L \quad (26)$$

$$D = \frac{1}{2} \rho U^2 c C_D \quad (27)$$

$$C_L = \begin{cases} a_0 + a_1 \alpha & \text{for } |\alpha| < \alpha_{stall} \\ A \sin 2(\alpha - \alpha_0) & \text{for } |\alpha| > \alpha_{stall} \end{cases} \quad (28)$$

$$C_D = \begin{cases} d_0 + d_1 \alpha + d_2 \alpha^2 & \text{for } |\alpha| < \alpha_{stall} \\ D + E \cos 2(\alpha - \alpha_0) & \text{for } |\alpha| > \alpha_{stall} \end{cases} \quad (29)$$

## References

**Abbott, I. H.; von Doenhoff, A. E.** (1949): *Theory of Wing Sections, Including a Summary of*

*Airfoil Data.* McGraw-Hill Book Co. Inc., New York.

**Cesnik, C. E. S.; Opoku, D. G.; Nitzsche, F.; Cheng, T.** (2004): Active twist rotor blade modelling using particle-wake aerodynamics and geometrically exact beam structural dynamics. *Journal of Fluids and Structures*, vol. 19, pp. 651–668.

**Chandiramani, N. K.; Plaut, R. H.; Librescu, L. I.** (1996): Non-linear flutter of a buckled shear-deformable composite panel in a high-supersonic flow. *ARL-CR-295*.

**Christov, I.; Christov, C. I.; Jordan, P. M.** (2007): Cumulative nonlinear effects in acoustic wave propagation. *CMES- Computer Modeling in Engineering and Sciences*, vol. 17, no. 1, pp. 47–54.

**Desceliers, C.; Soize, C.** (1999): Asymptotic treatment of the trapeze effect in finite element cross-sectional analysis of composite beams. *Int. J. Non-Linear Mech.*, vol. 34, pp. 709–721.

**Dowell, E. H.** (1990): Nonlinear Aeroelasticity. *AIAA-90-1031-CP*, pp. 1497–1507.

**Dowell, E. H.; Ilgamov, M.** (1988): Studies in Nonlinear Aeroelasticity. *Springer-Verlag*.

**Han, Z. D.; Rajendran, A. M.; Atluri, S. N.** (2005): Meshless Local Petrov-Galerkin (MLPG) approaches for solving nonlinear problems with large deformations and rotations. *CMES- Computer Modeling in Engineering and Sciences*, vol. 10, no. 1, pp. 1–12.

**Johnson, W.** (1975): *Helicopter Theory.* Princeton University Press.

**Kamakoti, R.; Lian, Y. S.; Regisford, S.; et al.** (2002): Computational aeroelasticity using a pressure-based solver. *CMES- Computer Modeling in Engineering and Sciences*, vol. 3, no. 6, pp. 773–789.

**Leishman, J. G.** (1992): *Principle of Helicopter Aerodynamics.* Cambridge University Press.

**Leu, S. Y.; Chen, J. T.** (2006): Sequential limit analysis of rotating hollow cylinders of nonlinear

isotropic hardening. *CMES- Computer Modeling in Engineering and Sciences*, vol. 14, no. 2, pp. 129–140.

**Librescu, L.; Chiochia, G.; Marzocca, P.** (1995): Implications of cubic physical aerodynamic non-linearities on the character of the flutter instability boundary. *Int. J. Non-Linear Mech.*, vol. 30, pp. 149–167.

**Liu, C. S.** (2006): The computations of large rotation through an index two nilpotent equation. *CMES- Computer Modeling in Engineering and Sciences*, vol. 16, no. 3, pp. 157–175.

**Patil, M. J.; Hodges, D. H.** (2004): On the importance of aerodynamic and structural geometrical nonlinearities in aeroelastic behavior of high-aspect-ratio wings. *Journal of Fluids and Structures*, vol. 19, pp. 905–915.

**Simonetti, F.; Marretta, R. M. A.** (2000): A numerical variational approach for rotor-propeller aerodynamics in axial flight. *CMES- Computer Modeling in Engineering and Sciences*, vol. 1, no. 3, pp. 81–90.

**Tang, D. M.; Dowell, E. H.** (1993): Nonlinear Aeroelasticity in Rotorcraft. *Mathl. Comput. Modelling*, vol. 18, pp. 157–184.

**Tang, D. M.; Dowell, E. H.** (2004): Effects of geometric structural nonlinearity on flutter and limit cycle oscillations of high-aspect-ratio wings. *Journal of Fluids and Structures*, vol. 19, pp. 291–306.

**Tongue, B. H.; Flowers, G.** (1988): Non-linear rotorcraft analysis. *Int. J. Non-Linear Mech.*, vol. 23, pp. 189–203.

**Wacher, A.; Givoli, D.** (2006): Remeshing and refining with moving finite elements, Application to nonlinear wave problems. *CMES- Computer Modeling in Engineering and Sciences*, vol. 15, no. 3, pp. 147–164.

## Appendix

### Flapping Equation for small flap angles

The three components of velocities are (Fig.1-2)

$$U_R = (\Omega R)\mu \cos \psi$$

$$U_T = (\Omega R)(r + \mu \sin \psi)$$

$$U_P = (\Omega R)(\lambda + r\beta^* + \mu\beta \cos \psi)$$

In this case, the following assumptions can be made

1. The out-of-plane component of velocity  $U_P$  is much smaller than the in-plane velocity  $U_T$ . So the resultant velocity is

$$U = \sqrt{U_T^2 + U_P^2} \approx U_T$$

2. The induced angle  $\phi$  is small, so that

$$\phi = \arctan \frac{U_P}{U_T} \approx \frac{U_P}{U_T}$$

3. As  $\phi$  is small and drag is at least one order of magnitude less than the lift,

$$F_z = L \cos \phi - D \sin \phi \approx L$$

Now considering a rigid articulated rotor blade with no flap hinge offset, the forces acting on an element of mass  $mdy$  with the assumptions for small  $\beta$ ,  $\cos \beta \approx 1$  and  $\sin \beta \approx \beta$ , are (see Fig.33),

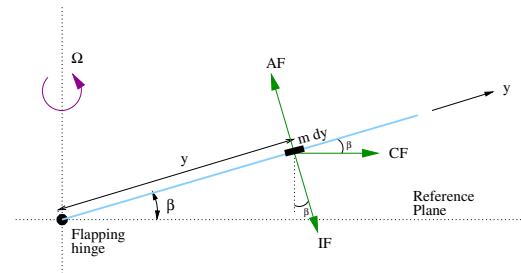


Figure 33: Forces acting on an element of a flapping blade

1. Inertial force (IF) =  $(mdy)\ddot{\beta}y$ , opposing the flapping motion;
2. Centrifugal force (CF) =  $(mdy)\Omega^2y$ , acting radially outwards; and
3. Aerodynamic force (AF) =  $Ldy$ , normal to the blade.

The moment equilibrium of the above forces about the flap hinge gives,

$$\int_0^R [(m dy) \ddot{\beta} y] y + \int_0^R [(m dy) \Omega^2 y] y \beta = \int_0^R [L dy] y$$

$$\text{i.e. } I_b (\ddot{\beta} + \Omega^2 \beta) = \int_0^R L y dy$$

$$\text{i.e. } \beta^{**} + \beta = \frac{R}{\Omega^2 I_b} \int_0^1 L r dr$$

This is the flapping equation for small flap angles. Typically, with this formulation, a linear aerodynamics model is considered, where  $C_L = C_{L_\alpha} \alpha$ ,  $C_{L_\alpha}$  being the lift-curve slope and drag is ignored.